

Synthesis, Structure, and Thiolysis Reactions of Pyridine Soluble Alkaline Earth and Yttrium Thiolates

Andrew P. Purdy,* Alan D. Berry, and Clifford F. George

Chemistry Division (Codes 6120 and 6170) and Laboratory for the Structure of Matter (Code 6030), Naval Research Laboratory, Washington D.C. 20375

Received January 15, 1997[⊗]

A series of alkaline earth thiolates, $M(\text{SR})_2$ ($M = \text{Ca}, \text{Sr}, \text{Ba}$), were synthesized from reactions between $M(\text{NH}_2)_2$ and RSH . For $\text{R} = \text{CMe}_3$, the products were only slightly soluble in pyridine, but the Ca derivative with $\text{R} = 1\text{-adamantyl}$ was soluble, and the Ca and Sr derivatives with $\text{R} = \text{CEt}_3$ were very soluble in pyridine. All the $\text{R} = \text{SCMe}_3$ derivatives dissolved in 1-methyl-2-pyrrolidinone (NMP). One yttrium thiolate, $(\text{Et}_3\text{SC})_2\text{Y}(\mu\text{-SCEt}_3\text{-Py}_2)_2$, was also prepared and characterized by single-crystal X-ray diffraction, as was $(\text{Sr}(\mu\text{-SCEt}_3)_2(\text{NH}_3)\text{Py})_n$. The former crystallized as discrete dimers with planar $(\text{YS})_2$ rings, and the latter formed an infinite chain of Sr atoms linked by thiolate bridges. Crystal data: $(\text{Et}_3\text{SC})_2\text{Y}(\mu\text{-SCEt}_3\text{Py}_2)_2$ $\text{P}\bar{1}$, $a = 11.592(1) \text{ \AA}$, $b = 17.328(2) \text{ \AA}$, $c = 18.376(2) \text{ \AA}$, $\alpha = 81.617(7)^\circ$, $\beta = 79.546(5)^\circ$, $\gamma = 78.169(7)^\circ$, and $Z = 2$; $(\text{Sr}(\mu\text{-SCEt}_3)_2(\text{NH}_3)\text{Py})_n$ $\text{P}2_1/c$, $a = 9.332(2) \text{ \AA}$, $b = 20.316(2) \text{ \AA}$, $c = 13.024(1) \text{ \AA}$, $\beta = 102.879(9)^\circ$, and $Z = 4$. Solutions of $\text{Ca}(\text{SCEt}_3)_2$ and $\text{Y}(\text{N}(\text{SiMe}_3)_2)_3$ or $(\text{Et}_3\text{SC})_2\text{Y}(\mu\text{-SCEt}_3\text{Py}_2)_2$ in pyridine were converted to gels or powders, respectively, by reaction with an excess of H_2S , and the solids were pressed into pellets and thermolyzed to CaY_2S_4 under flowing H_2S .

Introduction

There has been recent interest in ternary sulfides as two-color IR optical window materials¹ as well as other uses, such as phosphor materials.² Alkaline earth and lanthanide sulfide materials have been prepared by a variety of methods, including traditional solid state synthesis,³ solid state metathesis,⁴ sulfidization of oxides or carbonates,⁵ and sulfidization of alkoxides.⁶ Synthesis of lanthanum sulfide by sol-gel methods using $\text{La}(\text{N}(\text{SiMe}_3)_2)_3$ and H_2S has also been reported.⁷ Hydrolysis or sol-gel reactions using alkoxide precursors have been employed successfully for the synthesis of a wide variety of oxide materials,⁸ and analogous reactions using metal thiolates and H_2S are an obvious avenue of study. An obstacle to such work is the lack of soluble alkaline earth thiolates. Some very recent reports show alkaline earth thiolates with bulky aromatic ligands, such as $\text{SC}_6\text{H}_2(\text{CMe}_3)_3$ and $\text{SC}_6\text{H}_2\text{Ph}_3$, to be soluble in some organic solvents.⁹ As one might expect aromatic thiolate ligands to pyrolyze easily to carbon, we preferred to use tertiary aliphatic thiolates as molecular precursors. This work involves the synthesis of new alkaline earth and yttrium thiolates, crystal structures of $(\text{Sr}(\mu\text{-SCEt}_3)_2(\text{NH}_3)\text{Py})_n$ and $(\text{Et}_3\text{SC})_2\text{Y}(\mu\text{-SCEt}_3\text{-Py}_2)_2$, and the results of reactions between solutions of alkaline

earth and yttrium thiolates and silylamides and H_2S with subsequent thermolysis.

Experimental Section

General Comments. All manipulations were performed in a helium-filled Dri-Lab or on the vacuum line unless stated otherwise. The thick-walled H-tube and procedures used for reactions in liquid ammonia at room temperature were described earlier.¹⁰ H-tubes for thiol reactions were equipped with either 100 or 25 mL bulbs on each side, a stir bar was on the reaction bulb side, and a Kontes valve was positioned between the reaction bulb and the fine frit. The metals and YCl_3 were obtained from Alfa Products; THF, pyridine, potassium bis(trimethylsilyl)amide, *tert*-butanethiol, triethylcarbinol, 1-bromoadamantane, thiourea, ammonium thiocyanate, pyridine-*d*₅, 1-methyl-2-pyrrolidinone (NMP), and *p*-toluenesulfonic acid were obtained from Aldrich. All solvents were dried before use: pyridine was distilled from CaH_2 and kept over freshly activated 3 Å molecular sieves, THF was distilled from NaOCH_2 , toluene was distilled from sodium, and NMP (anhydrous grade) was stored over 3 Å molecular sieves. Ammonium thiocyanate was sublimed *in vacuo* before use. Metal amides ($M(\text{NH}_2)_n$) ($M = \text{Ca}, \text{Sr}, \text{Ba}, \text{K}$) were obtained from a reaction between the metal and large excess of anhydrous ammonia (Air Products) conducted in a stainless steel cylinder equipped with a suitable Hoke valve. Hydrogen sulfide (99.5%, CP) was obtained from Matheson and was used as received or dried over P_2O_5 , as stated in the discussion. A Lindberg 55035 furnace was used for temperatures up to 1100 °C, and a Thermcraft SiC tube furnace was used for higher temperatures. $\text{Y}(\text{N}(\text{SiMe}_3)_2)_3$ was made from YCl_3 and $\text{KN}(\text{SiMe}_3)_2$ in THF.¹¹ 1-Adamantanethiol and *tert*-heptanethiol were made by literature procedures.¹² The 1-adamantanethiol was contaminated with about 8% 1-bromoadamantane, but the latter did not react with metal amides and did not affect the reaction. NMR spectra were recorded on a Bruker AC-300 in $\text{C}_5\text{D}_5\text{N}$ unless indicated otherwise, and IR spectra were recorded on a Nicolet Magna-IR 750 FTIR instrument. SEM (scanning electron microscopy) photos were obtained on a Hitachi S-800 F.E. instrument at 25 kV. Samples were coated with evaporated carbon to insure conductivity. X-ray powder diffraction patterns were obtained with

[⊗] Abstract published in *Advance ACS Abstracts*, July 1, 1997.

- (1) (a) Lowe-Ma, C. K.; Vanderah, T. A.; Smith, T. E. *J. Solid State Chem.* **1995**, *117*, 363. (b) Kumta, P. N.; Risbud, S. H. *J. Mater. Sci.* **1994**, *29*, 1135.
- (2) Yuta, M. M.; White, W. B. *J. Electrochem. Soc.* **1992**, *139*, 2347.
- (3) Sleight, A. W.; Prewitt, C. T. *Inorg. Chem.* **1968**, *7*, 2282.
- (4) Cotter, J. P.; Fitzmaurice, J. C.; Parkin, I. P. *J. Mater. Chem.* **1994**, *4*, 1603.
- (5) (a) Tsai, M. S.; Hon, M. H. *Mater. Sci. Eng.* **1994**, *B26*, 29. (b) Tsai, M. S.; Wang, L. H.; Hon, M. H. *J. Am. Ceram. Soc.* **1995**, *78*, 1185. (c) Sokolov, V. V.; Kamarzin, A. A.; Trushnikova, L. N.; Savelyeva, M. V. *J. Alloys Comp.* **1995**, *225*, 567.
- (6) (a) Wang, L. H.; Hon, M. H. *Jpn. J. Appl. Phys., Part 1* **1992**, *31*, 2177. (b) Kumta, P. N.; Risbud, S. H. *J. Mater. Res.* **1993**, *8*, 1394.
- (7) Allen, G. C.; Paul, M.; Dunleavy, M. *Adv. Mater.* **1992**, *4*, 424.
- (8) Rao, C. N. R. *Mater. Sci. Eng.* **1993**, *B18*, 1.
- (9) (a) Ruhlandt-Senge, K. *Inorg. Chem.* **1995**, *34*, 3499. (b) Ruhlandt-Senge, K.; Davis, K.; Dalal, S.; Englich, U.; Senge, M. O. *Inorg. Chem.* **1995**, *34*, 2587. (c) Gindelberger, D. E.; Arnold, J. *Inorg. Chem.* **1994**, *33*, 6293. (d) Ellison, J. J.; Power, P. P. *Inorg. Chem.* **1994**, *33*, 4231.

(10) Purdy, A. P. *Inorg. Chem.* **1994**, *33*, 282.

(11) Bradley, D. C.; Ghotra, J. S.; Hart, F. A. *J. Chem. Soc., Dalton Trans.* **1973**, 1021.

(12) (a) Geigy, J. R. *Chem. Abstr.* **60**, 9167c. (b) Wolff, J. J.; Frenkins, G.; Harms, K. *Chem. Ber.* **1991**, *124*, 551.

Cu K α radiation on a Scintag XDS-2000 diffractometer equipped with a graphite monochromator and a scintillation detector. Elemental analyses were performed by E+R Microanalytical Laboratories, Inc., Corona, NY.

Synthesis of Ca(SAd)₂ (1). Calcium amide (1.0 g, 14 mmol) was combined with AdSH (4.8 g, 28 mmol) and ~40 mL of pyridine in a 100 mL H-tube and stirred for 72 h. The mixture was filtered, and product was washed through the frit with hot pyridine. The white solid obtained by recrystallization from hot pyridine was dried *in vacuo* at 100 °C, affording 4.1 g (80%) of Ca(SAd)₂. Anal. Found (Calcd) for C₂₀H₃₀S₂Ca: C, 63.94 (64.12); H, 7.93 (8.07); Ca, 10.58 (10.70). ¹H NMR: δ 2.24 (β -CH₂), 1.49 (δ -CH₂), 1.82 (CH). ¹³C NMR: δ 37.0 (β -CH₂), 31.3 (δ -CH₂), 51.3 (CH), 43.4 (C).

Synthesis of M(SCMe₃)₂ (2–4). Barium amide (0.671 g, 3.96 mmol) was transferred in a drybox to a dry Pyrex reactor (volume \approx 100 mL) equipped with a stir bar and a Kontes vacuum stopcock. Excess *t*-BuSH (dried over 4 Å molecular sieves) was vacuum-distilled into the reactor, and the mixture was warmed to ambient temperature. After a 2–3 min induction period, a faint bubbling was observed; no heat was evolved. After 10–15 min, the milky white suspension contained an area of yellow color. The reaction mixture was allowed to stir at ambient temperature overnight, and the excess *t*-BuSH was removed *in vacuo*. The off white solid was washed several times with THF in an H-tube to remove a small amount of a more soluble yellow material. The remaining off white residue was heated *in vacuo* at 60 °C to remove the last traces of NH₃ and THF. Yield: 1.23 g (98.2%). Anal. Found (Calcd) for C₈H₁₈S₂Ba: C, 30.21 (30.44); H, 5.62 (5.75); S, 20.02 (20.31); Ba, 43.54 (43.50). The Ca and Sr derivatives were prepared in a similar manner. Anal. Found (Calcd) for C₈H₁₈S₂Ca: C, 44.16 (43.99); H, 7.76 (8.31); S, 29.30 (29.36); Ca, 18.33 (18.35). Anal. Found (Calcd) for C₈H₁₈S₂Sr: C, 36.20 (36.13); H, 6.38 (6.82); S, 24.03 (24.1); Sr, 33.02 (32.94). ¹³C NMR (NMP + C₆D₆ + TMS): δ Ca-(SCMe₃)₂ 40.34 (Me), 38.62 (C); δ Sr(SCMe₃)₂ 40.27 (Me), 39.13 (C); δ Ba(SCMe₃)₂ 39.89 (Me), 41.01 (C).

Synthesis of Ca(SCEt₃)₂ (5). Calcium amide (1.15 g, 15.9 mmol), Et₃CSH (4.10 g, 31.0 mmol), and pyridine (15 mL) were combined in a 25 mL H-tube and stirred for 12 h. The mixture was filtered hot, and upon solvent removal, the solid would not redissolve in pyridine. The ammonia adduct appeared to be only sparingly soluble in pyridine. Filtration and drying *in vacuo* to 90 °C afforded solvent-free Ca(SCEt₃)₂ (4.40 g, 94%). Anal. Found (Calcd) for C₁₄H₃₀S₂Ca: C, 55.77 (55.57); H, 9.83 (9.99); Ca, 13.22 (13.25). ¹H NMR: δ 1.06 (CH₃, t), 1.71 (CH₂, q). ¹³C NMR: δ 10.23 (CH₃), 36.11 (CH₂), 52.22 (C).

Synthesis of Sr(SCEt₃)₂ (6). Strontium amide (1.14 g, 9.53 mmol) and Et₃CSH (2.53 g, 19.1 mmol) were combined with 20 mL of pyridine in an H-tube and stirred at 60 °C for 12 h. Hot filtration, followed by recrystallization from pyridine, afforded (Sr(μ -SCEt₃)₂(NH₃)Py)_n (**6a**), which was desolvated under dynamic vacuum at 90 °C for 12 h to Sr(SCEt₃)₂. Isolated yield: 1.91 g (57%). Anal. Found (Calcd) for C₁₄H₃₀S₂Sr: C, 47.96 (48.03); H, 8.62 (8.64); Sr, 24.74 (25.03). ¹H NMR: δ 1.08 (CH₃, br), 1.81 (CH₂, br). ¹³C NMR: δ 10.29 (CH₃), 36.29 (CH₂), 52.87 (C).

Synthesis of Y(NH₂)₃. A thick-walled H-tube equipped with flea stir bars on both sides was charged with Y (0.30 g, 3.4 mmol) and NH₄SCN (0.77 g, 10 mmol) on one side and KNH₂ (0.56 g, 10 mmol) on the other side. About 7 mL of NH₃ was condensed onto the thiocyanate mixture and 3 mL of NH₃ was condensed onto the KNH₂ at -196 °C. The yttrium dissolved over 12 h at 25 °C, and the Y(SCN)₃ solution was added to the KNH₂ solution with agitation. The mixture was filtered, and the solid was washed four times with recondensed solvent and dried *in vacuo*, affording Y(NH₂)₃ (0.39 g, (85%)). Anal. Found (Calcd) for YN₃H₆: N, 30.56 (30.68); H, 4.41 (4.42); Y, 64.86 (64.91). IR (KBr pellet): 3333, 3268 (NH stretch), 1519 (s, NH bend), 591 (vs).

Synthesis of ((Et₃SC)₂Y(μ -SCEt₃)₂Py)₂ (7). (a) Yttrium amide (0.24 g, 1.7 mmol), Et₃CSH (0.68 g, 5.2 mmol), and pyridine (10 mL) were combined in a 25 mL H-tube and heated at 50–60 °C for 4 days. The mixture was filtered hot, and the product was washed through the frit with recondensed solvent four times. After the solvent was removed at room temperature, the product was recrystallized from toluene; 520 mg of impure (based on ¹H and ¹³C NMR) product was isolated.

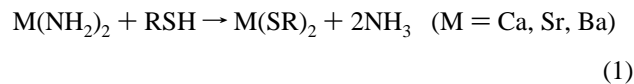
(b) Yttrium metal (1.0 g, 11 mmol) and Et₃CSH (4.5 g, 34 mmol) were combined in a 50 mL bulb in 20 mL of pyridine. Stirring for 24 h produced no reaction. Ammonia (21 mmol) was added at -196 °C, and the mixture was stirred at 50 °C for 10 days. All volatile materials were removed *in vacuo*, and the solids were mixed with warm toluene and filtered through a fine frit. The solvent was removed from the filtrate under vacuum, and the resulting solid was recrystallized from heptane-toluene to afford 0.40 g **7** (6%). Most of the metal did not react. Anal. Found (Calcd) for C₆₂H₁₁₀N₄S₆Y: C, 58.38 (58.10); H, 8.78 (8.65); N, 4.12 (4.37); S, 15.30 (15.01); Y, 13.91 (13.87). ¹H NMR: δ 1.00 (t, CH₃), 1.94 (q, CH₂). ¹³C NMR: δ 9.93 (CH₃), 34.8 (CH₂), 57.6 (C).

Thiolysis Reactions. One side of a 5 mL H-tube with a fine frit was charged with a pyridine solution of the precursors (Table 5). All noncondensable gases were pumped out of the tube by freeze-pump-thaw cycles, and an excess of H₂S was condensed into the empty side. The precursor solution was stirred as the H₂S was warmed and allowed to diffuse in. The mixture was allowed to stir for several hours to a day at ambient temperature, followed by a day at 90–100 °C. The solids were filtered, washed with recondensed solvent, and dried *in vacuo* at 110–160 °C. The powders or gelatinous precipitates produced were pressed into a pellet at 50 000 psi and heated in a tube furnace under H₂S flow. All transfers to the tube furnace were performed under inert atmosphere. Typically, one bubble every 1–2 sec passed through the exhaust bubbler (oil bubbler with 1/4 in. tubing). Additional conditions and amounts of reactants are stated in the discussion or Table 5.

Crystallographic Studies of 6a and 7. Suitable crystals of **6a** and **7** were mounted in thin-walled glass capillaries under He atmosphere; a small amount of pyridine was added to the capillary containing **6a**. Data were collected in the $\theta/2\theta$ mode on an automated Siemens P4 diffractometer equipped with an incident beam graphite monochromator (Mo K α , λ = 0.710 73) at 295 K. Data were corrected for Lorentz and polarization effects, and semi-empirical absorption corrections were applied. Maximum and minimum transmissions were 0.29 and 0.20 and 0.36 and 0.31, respectively, for **6a** and **7**. In each case, the structures were determined by direct methods and refined using full-matrix least-squares methods, as implemented by the program SHELXL. In all structures, the parameters refined included the coordinates and anisotropic thermal parameters for all but the hydrogen atoms. Hydrogen atoms were placed in idealized positions (C–H = 0.96 Å), and the coordinate shifts for carbon were applied to the bonded hydrogens. The isotropic thermal parameters for the hydrogens were fixed. In **6a**, several of the Et groups are disordered, and alternate positions for the terminal methyl groups were refined with occupancies of ca. 50%.

Results and Discussion

Synthesis and Characterization. The alkaline earth thiolates M(SR)₂ were prepared from a reaction between M(NH₂)₂ and the thiol, either neat or in pyridine solution (eq 1). An ammonia



complex of the thiolate was initially formed, which was desolvated by gentle heating under vacuum. The thiolates with R = CMe₃ were only very slightly soluble in pyridine but proved to be very soluble in a more polar solvent, 1-methyl-2-pyrrolidinone (NMP). Thiolates with R = 1-adamantyl (Ad) were slightly soluble, and those with R = CEt₃ were very soluble in pyridine. None of the alkaline earth thiolates were soluble

Table 1. Thermal Decomposition of Thiolates

compound	onset temp, °C	volatile products (mol %) ^a	solid product, ^c phase, appearance
Ca(SAd) ₂ (1)	315	Ad ₂ S (41), AdSH (27), AdH (31) ^d	CaS, black carbonized
Ca(SCMe ₃) ₂ (2)	170	Me ₂ C=CH ₂ (45), Me ₃ CSH (53), Me ₃ CH(1), (Me ₃ CS) ₂ (<1), (Me ₃ C) ₂ S (<1)	CaS, grey
Sr(SCMe ₃) ₂ (3)	170	Me ₂ C=CH ₂ (48), Me ₃ CSH (45), Me ₃ CH (4), H ₂ S (3), (Me ₃ CS) ₂ (<1), (Me ₃ C) ₂ S (<1)	SrS, grey
Ba(SCMe ₃) ₂ (4)	175	Me ₂ C=CH ₂ (45), Me ₃ CSH (52), Me ₃ CH (3), (Me ₃ C) ₂ S (<1), (Me ₃ CS) ₂ (<1)	BaS, grey
Ca(SCEt ₃) ₂ (5)	175	Et ₂ C=C(H)Me (55), Et ₃ CSH (44), H ₂ S (1)	CaS, off white
Sr(SCEt ₃) ₂ (6)	175	Et ₂ C=C(H)Me (53), Et ₃ CSH (43), Et ₃ CH (2), H ₂ S (1)	SrS, grey
Y(SCEt ₃) ₃ Py ₂ (7)	70	Et ₂ C=C(H)Me (45), Et ₃ CSH (29), H ₂ S (4), Py (22)	amorphous, brown ^b

^a Amount determined by ¹H NMR integration. ^b Black, poorly crystalline Y₂S₃ after heating to 800 °C. ^c Heated to 475 °C. Phases identified by powder X-ray diffraction. ^d A small amount of unidentified product is present.

in THF. Although the CEt₃ thiolates were very soluble in pyridine, their ammonia complexes had a much lower solubility, which aided their recrystallization and isolation. This low solubility of NH₃ adducts may be due to formation of a polymeric structure, such as that which forms for (Sr(μ -SCEt₃)₂(NH₃)Py)_n (**6a**). The room-temperature proton NMR spectrum of **5** in C₅D₅N showed a fairly sharp splitting pattern for the ethyl groups, but the spectra of **6** and the adamantyl compound **1** had broad lines with no observable splitting.

A yttrium thiolate, ((Et₃SC)₂Y(μ -SCEt₃)₂Py)₂ (**7**), was also synthesized by the reaction of the thiol with yttrium amide or with the metal in the presence of ammonia. This synthesis proved to be more troublesome than the syntheses of **1–6** as the low thermal stability of Y(SCEt₃)₃ necessitated keeping the temperature below 60 °C during the synthesis, and the isolated yields were low. Excessive heating of the reaction mixture caused peaks for a large number of unidentified decomposition products to appear in the NMR spectrum. The initial product of the synthesis reaction was an ammonia adduct of low solubility, and attempts to filter a hot solution resulted in substantial decomposition. A better procedure was to remove the solvent first and redissolve the product before filtration. Thermal instability also prevented desolvation to Y(SCEt₃)₃.

The thiolates with tertiary alkyl substituents began to decompose thermally at lower temperatures than the adamantyl derivative (Table 1). Although evolution of thiol and alkene began around 100 °C, the gas evolution was brief and no further emission occurred until closer to 200 °C. The initial emission of thiol and alkene occurred simultaneously with the loss of the last remaining traces of wash solvent and may have been due to the loss and possible decomposition of coordinated thiol. For this reason, the second emission of thiol and alkene was taken as the onset of decomposition for **2–6** in Table 1. Solution NMR spectra were taken of the solids before and after heating to about 130–150 °C and above the onset of decomposition. The ¹³C NMR spectra of the *tert*-butylthiolates **2–4** (in NMP) showed only slight chemical shift changes on heating to 130–150 °C, and the ¹H and ¹³C spectra of the *tert*-heptylthiolates (in C₅D₅N) showed no change at all. Samples of SCMe₃ compounds **2–4** heated to 220 °C and held there until gas evolution ceased remained soluble (Ca) or partially soluble (Sr, Ba) in NMP, but SCEt₃ compounds **5** and **6** became insoluble in NMP and pyridine. The ¹³C NMR spectra of NMP solutions of partially decomposed **2–4** had substantial chemical shift changes but still showed the presence of only one magnetically equivalent CMe₃ group, possibly due to rapid exchange. Most of the decomposition for the tertiary alkyl derivatives **2–6** did not occur until temperatures above 240 °C were reached. The yttrium complex **7** decomposed in several stages, from which gas evolution was almost complete by 185 °C. Compounds **2–7** decomposed mainly by alkene and thiol

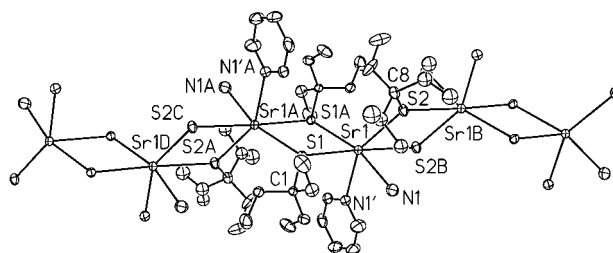


Figure 1. Structure of (Sr(μ -SCEt₃)₂(NH₃)Py)_n (**6a**), six repeat units shown. Pyridine carbons and CEt₃ groups on several repeat units omitted for clarity. Thermal ellipsoids are at the 20% probability level.

elimination, similar to the decomposition of tertiary alkoxides,¹³ but the Me₃C compounds emitted small amounts of alkane, sulfide, and disulfide as well (Table 1). In contrast, the adamantyl compound **1** eliminated mainly Ad₂S. The decomposition of thiolates by elimination of R₂S has been previously reported.^{14,16a} Although the SCR₃ compounds decomposed rather cleanly, with only traces of organic residues in the inorganic product, **1** formed a highly carbonized product. None of the thiolates sublimed under vacuum.

Structure Descriptions. We were not able to obtain crystals of unsolvated thiolates, but crystals of some solvated *tert*-heptylthiolates were obtained. The structure of the ammonia, pyridine adduct of **6** ((Sr(μ -SCEt₃)₂(NH₃)Py)_n (**6a**)) consists of an infinite chain of (SrS)₂ rings linked at Sr, as depicted in Figure 1. Crystal data are listed in Table 2, and bond lengths and angles are listed in Table 3. Each asymmetric unit consists of one Sr(SCEt₃)₂(NH₃)Py moiety from which the rest of the chain is generated by a series of inversion and inversion plus cell translation operations. The centrosymmetric rings are planar and alternate between rings of two slightly different dimensions.

- (13) (a) Bradley, D. C.; Faktor, M. M. *J. Appl. Chem.* **1959**, 435. (b) Bradley, D. C.; Faktor, M. M. *Trans. Faraday Soc.* **1959**, 55, 2117. (c) Nandi, M.; Rubright, D.; Sen, A. *Inorg. Chem.* **1990**, 29, 3066. (d) Dongare, M. K.; Sinha, A. P. B. *Thermochim. Acta.* **1982**, 57, 37. (14) Cheng, Y.; Emge, T. J.; Brennan, J. G. *Inorg. Chem.* **1996**, 35, 342. (15) Brewer, M.; Lee, J.; Brennan, J. G. *Inorg. Chem.* **1995**, 34, 5919. (16) (a) Lee, J.; Brewer, M.; Berardini, M.; Brennan, J. G. *Inorg. Chem.* **1995**, 34, 3215. (b) Nief, F.; Ricard, L. *J. Chem. Soc., Chem. Commun.* **1994**, 2723. (c) Mashima, K.; Nakayama, Y.; Fukumoto, H.; Kanehisa, N.; Kai, Y.; Nakamura, A. *J. Chem. Soc., Chem. Commun.* **1994**, 2523. (d) Mashima, K.; Shibahara, T.; Nakayama, Y.; Nakamura, A. *J. Organomet. Chem.* **1995**, 501, 263. (e) Stults, S. D.; Andersen, R. A.; Zalkin, A. *Organometallics* **1990**, 1623. (f) Brewer, M.; Khasnis, D.; Buretea, M.; Berardini, M.; Emge, T. J.; Brennan, J. G. *Inorg. Chem.* **1994**, 33, 2743. (g) Mashima, K.; Nakayama, Y.; Kanehisa, N.; Kai, Y.; Nakamura, A. *J. Chem. Soc., Chem. Commun.* **1993**, 1847. (h) Cetinkaya, B.; Hitchcock, P. B.; Lappert, M. F.; Smith, R. G. *J. Chem. Soc., Chem. Commun.* **1992**, 932. (i) Aspinall, H. C.; Bradley, D. C.; Hursthouse, M. B.; Sales, K. D.; Walker, N. P. C. *J. Chem. Soc., Chem. Commun.* **1985**, 1585. (j) Tatsumi, K.; Ameniya, T.; Kawaguchi, H.; Tani, K. *J. Chem. Soc., Chem. Commun.* **1993**, 773.

Table 2. Crystal and Refinement Data

	6a	7
formula	[Sr(SCEt ₃) ₂ (NH ₃)Py] _n	[Y(SCEt ₃) ₂ Py ₂] ₂
space group	P2 ₁ /c (No. 14)	P1̄ (No. 2)
a, Å	9.332(2)	11.592(1)
b, Å	20.316(2)	17.328(2)
c, Å	13.024(1)	18.376(2)
α, deg	90.0	81.617(7)
β, deg	102.879(9)	79.546(5)
γ, deg	90.0	78.169(7)
V, Å ³	2407.1(5)	3529.8(6)
Z	4	2
λ, Å	0.71073	0.71073
T, °C	22	22
fw	446.25	1279.7
ρ(calcd), g cm ⁻³	1.231	1.204
μ, abs coeff, mm ⁻¹	2.417	1.850
R, wR2 (obs), wR2 (all) ^a	0.066, 0.096, 0.123	0.076, 0.120, 0.163

^a $R = \sum |F_o - F_c| / \sum |F_o|$ (**6a**); $w = 1/[\sigma^2(F_o^2) + (0.0104P)^2 + 5.4099P]$, where $P = (F_o^2 + 2F_c^2)/3$ (**7**); $w = 1/[\sigma^2(F_o^2) + (0.0383P)^2 + 3.3509P]$; $wR2 = [\sum(w(F_o^2 - F_c^2)^2) / \sum(w(F_o^2)^2)]^{1/2}$.

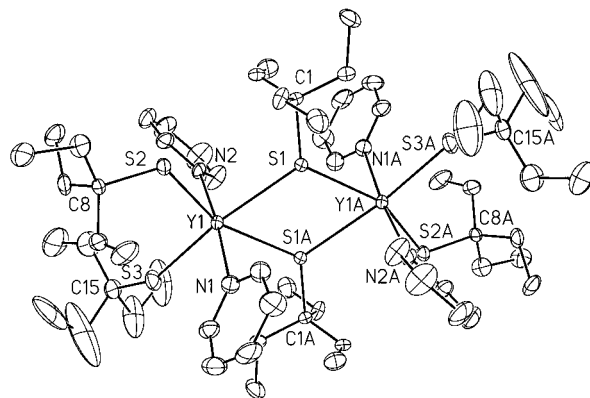
Table 3. Selected Bond Lengths (Å) and Angles (deg) for **6a**^a

Sr(1)–N(1)	2.725(7)	Sr(1)–S(2)B	3.019(3)
Sr(1)–N(1')	2.745(7)	Sr(1)–S(1)	3.019(3)
Sr(1)–S(1)A	2.980(2)	S(1)–C(1)	1.856(8)
Sr(1)–S(2)	3.010(3)	S(2)–C(8)	1.868(9)
N(1)–Sr(1)–N(1')	81.4(3)	N(1')–Sr(1)–S(1)	92.4(2)
N(1)–Sr(1)–S(1)A	164.8(2)	S(1)A–Sr(1)–S(1)	72.94(8)
N(1')–Sr(1)–S(1)A	88.9(2)	S(2)–Sr(1)–S(1)	107.79(7)
N(1)–Sr(1)–S(2)	75.2(2)	S(2)B–Sr(1)–S(1)	173.66(8)
N(1')–Sr(1)–S(2)	150.3(2)	C(1)–S(1)–Sr(1)A	121.1(3)
S(1)A–Sr(1)–S(2)	117.39(8)	C(1)–S(1)–Sr(1)	121.4(3)
N(1)–Sr(1)–S(2)B	78.3(3)	Sr(1)A–S(1)–Sr(1)	107.06(7)
N(1')–Sr(1)–S(2)B	88.8(2)	C(8)–S(2)–Sr(1)	120.4(3)
S(1)A–Sr(1)–S(2)B	113.33(7)	C(8)–S(2)–Sr(1)B	128.2(3)
S(2)–Sr(1)–S(2)B	68.90(8)	Sr(1)–S(2)–Sr(1)B	111.10(8)
N(1)–Sr(1)–S(1)	95.7(2)		

^a Symmetry transformations used to generate equivalent atoms: A $-x+1, -y, -z$; B $-x, -y, -z$.

The Sr1–S1–Sr1A–S1A ring has angles of 107.06(7)° at sulfur and 72.94(8)° at Sr, while the Sr1–S2–Sr1B–S2B ring has angles of 111.10(8)° at S and 68.90(8)° at Sr. A line connecting the Sr centers would zigzag with angles of 144.5°, and the dihedral angle between the (SrS)₂ planes is 67.9°. There are four different Sr–S bonds ranging from 2.980(2) to 3.019(3) Å, which are slightly longer than the Sr–S bonds of 2.951(2) Å in Sr(SMes*)₂(THF)₄.^{9b} These slightly longer bonds are probably due to each SR ligand bridging two Sr atoms in **6a**. In both Sr(Mes*)₂(THF)₄ and **6a**, the Sr atoms are six-coordinate. The Sr–S–C angles range from 120.4(3)° to 128.2(3)° and are similar to the Sr–S–C angle of 120.9(3)° reported for Sr(SMes*)₂(THF)₄.

The structure of the yttrium thiolate ((Et₃SC)₂Y(μ-SCEt₃)Py₂)₂ (**7**) is illustrated in Figure 2, and selected bond lengths and angles are listed in Table 4. There are two independent molecules in the unit cell. In each of the molecules the dimeric (YS)₂ rings are centered on inversion centers and are, therefore, planar, and the yttrium atoms have a distorted octahedral geometry, with the SR groups in the equatorial positions and the pyridine ligands in the axial positions. The YS₄ moieties are nearly planar, and the sum of S–Y–S angles around the yttrium being 360.28° and 360.06°, and the N–Y–N angles of 174.8(4)° and 175.8(3)° and the N–Y–S angles of 85.0(2)–95.6(3)° are close to the 180° and 90°, respectively, of a perfect octahedron. As expected, the Y–S distances between Y and the bridging SR ligands of 2.825(3)–2.870(3) Å are significantly longer than the Y–S distances to the terminal ligands of 2.587-

**Figure 2.** Structure of ((Et₃SC)₂Y(μ-SCEt₃)Py₂)₂ (**7**), only one of two independent molecules shown. Thermal ellipsoids are at the 20% probability level.**Table 4.** Selected Bond Lengths (Å) and Angles (deg) for **7**^a

Y(1)–N(2)	2.478(9)	S(1)–C(1)	1.886(10)	Y(1')–S(2')	2.650(3)
Y(1)–N(1)	2.480(10)	S(2)–C(8)	1.857(10)	Y(1')–S(1')	2.825(3)
Y(1)–S(3)	2.587(3)	S(3)–C(15)	1.824(13)	Y(1')–S(1')B	2.870(3)
Y(1)–S(2)	2.681(3)	Y(1')–N(1')	2.472(9)	S(1')–C(1')	1.867(10)
Y(1)–S(1)A	2.848(3)	Y(1')–N(2')	2.492(9)	S(2')–C(8')	1.847(11)
Y(1)–S(1)	2.850(3)	Y(1')–S(3')	2.642(3)	S(3')–C(15')	1.860(11)
N(2)–Y(1)–N(1)	174.8(4)	N(1')–Y(1')–N(2')	175.8(3)		
N(2)–Y(1)–S(3)	88.0(2)	N(1')–Y(1')–S(3')	89.6(2)		
N(1)–Y(1)–S(3)	86.9(3)	N(2')–Y(1')–S(3')	90.9(2)		
N(2)–Y(1)–S(2)	92.1(3)	N(1')–Y(1')–S(2')	90.8(2)		
N(1)–Y(1)–S(2)	88.1(2)	N(2')–Y(1')–S(2')	85.0(2)		
S(3)–Y(1)–S(2)	101.54(10)	S(3')–Y(1')–S(2')	101.03(10)		
N(2)–Y(1)–S(1)A	94.3(2)	N(1')–Y(1')–S(1')	94.2(2)		
N(1)–Y(1)–S(1)A	87.7(2)	N(2')–Y(1')–S(1')	87.2(2)		
S(3)–Y(1)–S(1)A	102.48(10)	S(3')–Y(1')–S(1')	154.30(9)		
S(2)–Y(1)–S(1)A	155.33(9)	S(2')–Y(1')–S(1')	104.32(9)		
N(2)–Y(1)–S(1)	89.6(2)	N(1')–Y(1')–S(1')B	88.7(2)		
N(1)–Y(1)–S(1)	95.6(3)	N(2')–Y(1')–S(1')B	95.4(2)		
S(3)–Y(1)–S(1)	168.94(10)	S(3')–Y(1')–S(1')B	88.15(9)		
S(2)–Y(1)–S(1)	89.33(9)	S(2')–Y(1')–S(1')B	170.81(9)		
S(1)A–Y(1)–S(1)	66.93(9)	S(1')–Y(1')–S(1')B	66.56(9)		
Y(1)A–S(1)–Y(1)	113.07(9)	Y(1')–S(1')–Y(1')B	113.44(9)		

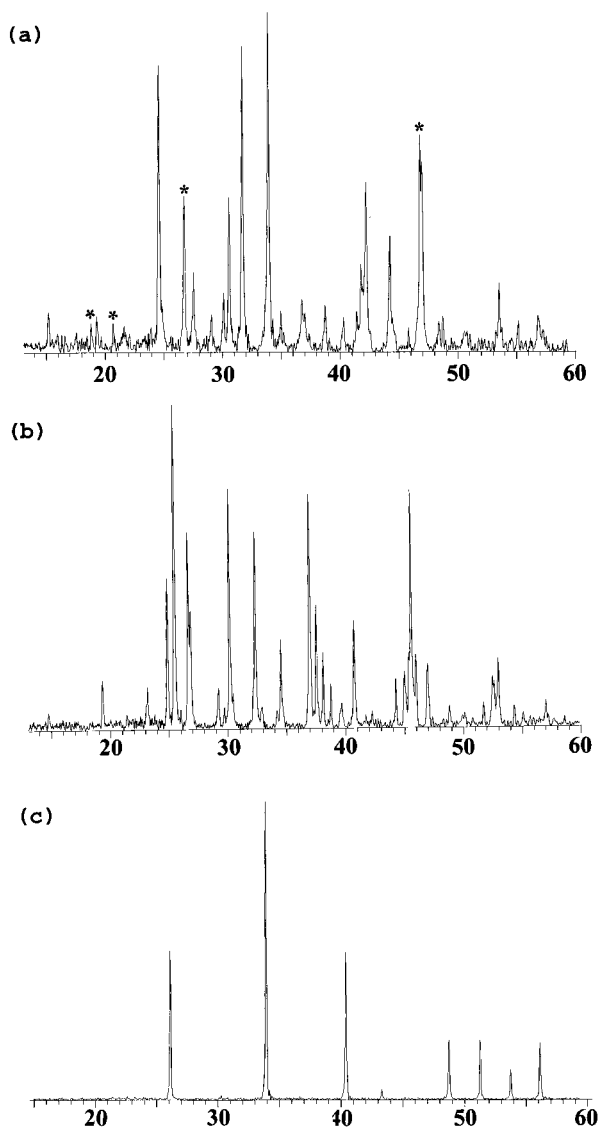
^a Symmetry transformations used to generate equivalent atoms: A $-x, -y+2, -z$; B $-x+1, -y+1, -z+1$.

(3)–2.681(3) Å. Although structurally characterized yttrium thiolates have not been previously reported, thiolates of yttrium, gadolinium, samarium, thulium, cerium, and lutetium have.¹⁶ Of the latter, Tm³⁺ (0.87 Å) and Yb³⁺ (0.858 Å) have the closest ionic radii to Y³⁺ (0.893 Å). A monomeric thiolate^{16a} Yb(SPh)₃Py₃ has average Yb–S bonds of 2.648 Å, which is within the range observed for the terminal Y–S bonds in **7**. Bridging SPh ligands to Yb in a Yb²⁺ complex (Yb(SPh)(Me₄C₄P)(THF)₂)₂^{16b} have Yb–S bonds of 2.789–2.833 Å and are similar to those in **7**. So far, the only lanthanide thiolate complexes reported with both bridging and terminal SR ligands have been the divalent Sm compound [Sm(SAr)(μ-SAr)(THF)₃]₂ and the analogous Eu²⁺ complex.^{16c} In the latter two Ln²⁺ compounds, average bridging Ln–S distances are 0.109 and 0.118 Å longer than the distance to their respective terminal SR ligands. In **7**, the average bridging Y–S bond is longer by 0.208 Å.

Internal S–Ln–S angles in (LnS)₂ rings vary from 63.60° to 78.94° and do not appear to correlate with ion size. The S–Y–S angles of 66.56(9)° and 66.93(9)° of **7** fall within that range. The Ln³⁺–S–C angles in complexes with monodentate SR ligands are typically around 120° ± 10°, with some exceptions possibly due to unusual coordination environments or steric constraints.¹⁶ Compound **7** has Y–S–C angles of 120.6(3)–124.2(3)° for the bridging SCEt₃ ligands and 121.4(4)–145.6(5)° for the terminal SCEt₃ ligands. The greater

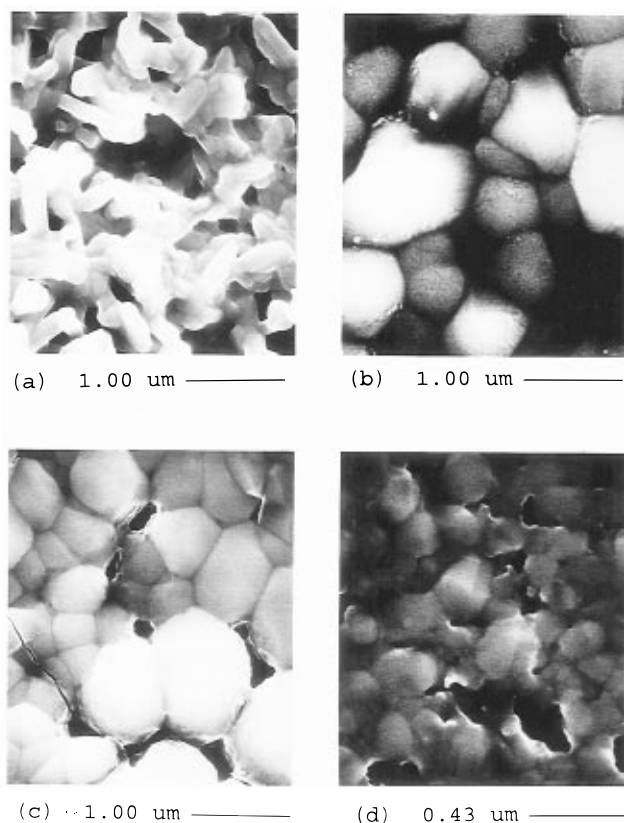
Table 5. Thiolytic Reactions in Pyridine Solution

precursors		H ₂ S	products	
metal compounds			sample	1000–1100 °C, H ₂ S flow, appearance, phases (XRD)
Y(SCEt ₃) ₃ Py ₂ 0.25 mmol		6.9 mmol	A	light grey CaY ₂ S ₄
Ca(SCEt ₃) ₂ 0.125 mmol				
NH ₃ 6.9 mmol				
Y(N(SiMe ₃) ₂) ₃ 0.88 mmol		6.3 mmol	B	tan CaY ₂ S ₄
Ca(SCEt ₃) ₂ 0.44 mmol				
Y(N(SiMe ₃) ₂) ₃ 0.88 mmol		6.9 mmol	C	dark grey, shiny SrY ₂ S ₄
Sr(SCEt ₃) ₂ 0.44 mmol				
Y(N(SiMe ₃) ₂) ₃ 0.88 mmol		6.9 mmol	D	grey, cubic Ca–Y–S Th ₃ P ₄ -type phase, <i>a</i> = 8.350(2) Å
Ca(SCEt ₃) ₂ 0.25 mmol				
Y(N(SiMe ₃) ₂) ₃ 0.83 mmol		2.7 mmol	E	Y ₂ S ₃ , cubic Ca–Y–S
Ca(SCEt ₃) ₂ 0.090 mmol				

**Figure 3.** X-ray powder patterns of (a) sample **B**, (b) sample **C**, (c) sample **D**. Peaks marked with asterisk (*) are unidentified.

variation in the terminal Y–S–C angles may be due to steric interactions or packing forces.

Thiolytic Reactions. Sol-gel experiments to synthesize ternary sulfides were performed by adding an excess of H₂S gas to a pyridine solution of the precursors. A representative list of experiments is presented in Table 5. The products were filtered, dried *in vacuo*, and thermolyzed to inorganic materials. When **7** was used as the yttrium source, the product was a white precipitate, but when Y(N(SiMe₃)₂)₃ was used, the reaction product was a white suspension which afforded a yellowish

**Figure 4.** SEM photographs of ternary sulfide materials: (a) sample **A**, 1040 °C, (b) sample **A**, sintered 1250 °C, (c) sample **B**, 1150 °C, (d) sample **C**, 1100 °C.

translucent gel upon filtration. Infrared spectra of vacuum dried gels/precipitates showed the presence of coordinated or solvated pyridine. The samples were heated under dynamic vacuum at 110–150 °C, which removed most but not all of the pyridine.

The nature of the product formed from thermolysis was highly dependent on the conditions used. Typically, the thiolytic product was pressed into a pellet and heated under H₂S flow. It was important to remove most of the absorbed pyridine by heating *in vacuo* prior to pressing into a pellet in order to avoid substantial carbonization. Excessive heating rates in the 200–600 °C range led to cracking and black, carbonized products; generally, heating rates of 6–8 °C/min were used. Higher flow rates of H₂S appeared to improve the purity of the product, as judged by a lighter color and a lower level of IR absorbing impurities in the 800–1600 cm⁻¹ region. For a given flow rate, a smaller diameter furnace tube appeared to produce better results, probably by increasing the actual flow over the pellet.

Slow heating of the pellets to 600 °C, followed by several hours at 1000–1100 °C resulted in fragile, relatively crack-

free, tan- to grey-coated CaY_2S_4 and SrY_2S_4 materials. The X-ray powder patterns of the CaY_2S_4 and SrY_2S_4 materials (Figure 3) showed minor impurity phases, which were not identified.^{1a} A calcium-deficient cubic phase¹⁷ (Th_3P_4 -type) was also produced with a Y:Ca precursor ratio of 3.5:1. No crystalline impurities were detected in the powder pattern of the latter (Figure 3). SEM photos show the particle sizes of all these materials to be in the micron range (Figure 4). The samples heated at 1250 °C were sintered but contained a number of pores (Figure 4b). A substantial amount of grain growth and densification occurred between 1040 and 1250 °C, see Figure 4a and b. The 1250 °C samples were darker in color than those heated to 1100 °C, possibly due to sulfur loss. Sintering at 1400 °C under H_2S flow turned CaY_2S_4 brown and opaque to IR. Infrared spectra of the sintered pellets (Figure 5) showed substantial IR absorbing impurities at 830 and 1040–1230 cm^{-1} for the $\text{Y}(\text{N}(\text{SiMe}_3)_2)_3$ -derived materials, which is most likely due to silicate.¹⁸ When **7** was used as the yttrium precursor, those large impurity peaks were absent but a smaller peak at 1100 cm^{-1} could be attributed to sulfate. The impurity absorptions at 1400 and 1540 cm^{-1} were observed to increase on exposure to the atmosphere and are assigned to carbonate. Drying the H_2S over P_2O_5 had little effect on these IR absorbing impurities. However, IR transmission losses from scattering are readily apparent in all the materials and may be due to a combination of excessively large particle size, material porosity, and the anisotropic structure^{1a} of CaY_2S_4 and SrY_2S_4 .

Conclusions. We have demonstrated that alkaline earth thiolates with bulky tertiary alkyl groups are soluble in pyridine

- (17) (a) Flathut, J.; Domange, L.; Patrie, M. *C. R. Acad. Sci. Paris*, **1960**, 2535. (b) Flathut, J.; Domange, L.; Patrie, M.; Bostsarron, A.; Guittard, M. *Adv. Chem. Ser.* **1963**, 39, 179.
 (18) Nyquist, R. A.; Kagel, R. O. *Infrared Spectra of Inorganic Compounds*; Academic Press Inc. San Diego, CA, 1971.

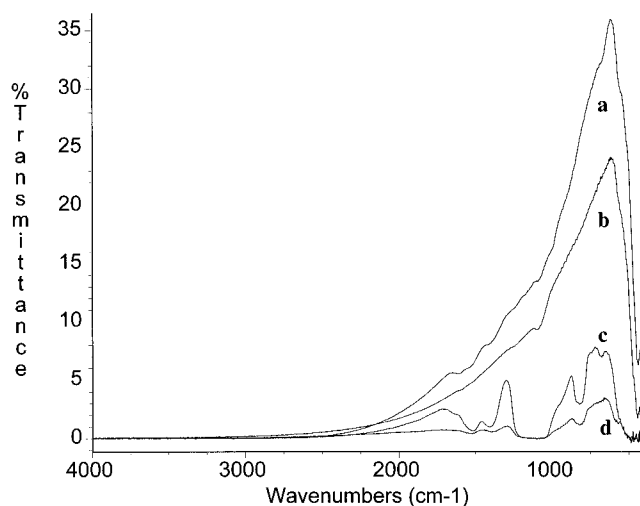


Figure 5. FTIR transmission spectra of ternary sulfide pellets: (a) sample **A** (0.14 mm thick), (b) sample **A**, sintered 1250 °C (0.12 mm thick), (c) sample **B** (0.48 mm thick), (d) sample **C** (0.41 mm thick). and NMP and can decompose rather cleanly to their respective metal sulfides. Furthermore, ternary sulfide materials can be synthesized in a manner analogous to the sol-gel processes commonly used for oxides, using thiolates and H_2S instead of alkoxides and H_2O . However, with sulfide materials one cannot “burn out” impurities the way one can with oxides; thus, preparing materials from thiolate precursors for optical applications remains a challenge.

Acknowledgment. We thank the ONR for financial support.

Supporting Information Available: Two X-ray crystallographic files, in CIF format are available. Access information is given on any current masthead page.

IC970045+